



# Allogeneic Cell Combination Therapy Ameliorates Chronic Kidney Disease-Induced Heart Failure with Preserved Ejection Fraction

Angela C. Rieger<sup>1</sup>, Bryon A. Tompkins<sup>1,2</sup>, Makoto Natsumeda<sup>1, </sup>, Victoria Florea<sup>1</sup>,  
Monisha N. Banerjee<sup>1,2</sup>, Jose Rodriguez<sup>1</sup>, Marcos Rosado<sup>1</sup>, Valeria Porras<sup>1</sup>, Krystalenia Valasaki<sup>1</sup>,  
Lauro M. Takeuchi<sup>1</sup>, Kevin Collon<sup>3</sup>, Sohil Desai<sup>1</sup>, Michael A. Bellio<sup>1</sup>, Aisha Khan<sup>1</sup>,  
Nilesh D. Kashikar<sup>4</sup>, Ana Marie Landin<sup>5</sup>, Darrell V. Hardin<sup>1</sup>, Daniel A. Rodriguez<sup>1,6</sup>,  
Wayne Balkan<sup>1,7, </sup>, Joshua M. Hare<sup>1,7</sup>, Ivonne Hernandez Schulman<sup>1,8,\*</sup>

<sup>1</sup>Interdisciplinary Stem Cell Institute, University of Miami Miller School of Medicine, Miami, FL, USA

<sup>2</sup>Department of Surgery, University of Miami Miller School of Medicine, Miami, FL, USA

<sup>3</sup>Department of Orthopedic Surgery, Keck School of Medicine of University of Southern California, Los Angeles, CA, USA

<sup>4</sup>Aurora Diagnostics GPA Laboratories (ADXGPA), Greensboro, NC, USA

<sup>5</sup>Cell Therapy and Vaccine Lab, Moffitt Cancer Center, Tampa, FL, USA

<sup>6</sup>Bascom Palmer Eye Institute, University of Miami Miller School of Medicine, Miami, FL, USA

<sup>7</sup>Cardiovascular Division, Department of Medicine, University of Miami Miller School of Medicine, Miami, FL, USA

<sup>8</sup>Katz Family Division of Nephrology and Hypertension, Department of Medicine, University of Miami Miller School of Medicine, Miami, FL, USA

\*Corresponding author: Ivonne H. Schulman, MD, Program Director, Translational and Clinical Studies of Acute Kidney Injury, Division of Kidney, Urologic and Hematologic Diseases (KUH), National Institutes of Health (NIH), National Institute of Diabetes and Digestive and Kidney Diseases (NIDDK), Two Democracy Plaza, Room #6077, 6707 Democracy Blvd, Bethesda, MD 20892-5458, USA. Tel: 301-435-3350; Mobile: 301-385-5744; Fax: 301-480-3510, Email: [ischulman@med.miami.edu](mailto:ischulman@med.miami.edu), [ivonne.schulman@nih.gov](mailto:ivonne.schulman@nih.gov)

## Abstract

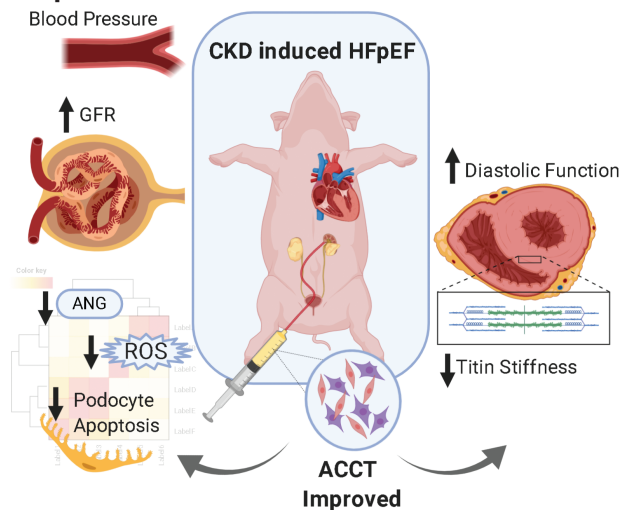
**Background:** Left ventricular hypertrophy and heart failure with preserved ejection fraction (HFpEF) are primary manifestations of the cardiorenal syndrome in patients with chronic kidney disease (CKD). Therapies that improve morbidity and mortality in HFpEF are lacking. Cell-based therapies promote cardiac repair in ischemic and non-ischemic cardiomyopathies. We hypothesized that cell-based therapy ameliorates CKD-induced HFpEF.

**Methods and Results:** Yorkshire pigs ( $n = 26$ ) underwent 5/6 embolization-mediated nephrectomy. CKD was confirmed by increased creatinine and decreased glomerular filtration rate (GFR). Mean arterial pressure (MAP) was not different between groups from baseline to 4 weeks. HFpEF was evident at 4 weeks by increased LV mass, relative wall thickening, end-diastolic pressure, and end-diastolic pressure-volume relationship, with no change in ejection fraction (EF). Four weeks post-embolization, allogeneic (allo) bone marrow-derived mesenchymal stem cells (MSC;  $1 \times 10^7$  cells), allo-kidney-derived stem cells (KSC;  $1 \times 10^7$  cells), allo-cell combination therapy (ACCT; MSC + KSC; 1:1 ratio; total =  $1 \times 10^7$  cells), or placebo (Plasma-Lyte) was delivered via intra-renal artery. Eight weeks post-treatment, there was a significant increase in MAP in the placebo group ( $21.89 \pm 6.05$  mmHg) compared to the ACCT group. GFR significantly improved in the ACCT group. EF, relative wall thickness, and LV mass did not differ between groups at 12 weeks. EDPVR improved in the ACCT group, indicating decreased ventricular stiffness.

**Conclusions:** Intra-renal artery allogeneic cell therapy was safe in a CKD swine model manifesting the characteristics of HFpEF. The beneficial effect on renal function and ventricular compliance in the ACCT group supports further research of cell therapy for cardiorenal syndrome.

**Key words:** chronic kidney disease (CKD); heart failure with preserved ejection fraction (HFpEF); cardiorenal; allogeneic cell combination therapy; cell-based therapy; mesenchymal stem cells (MSCs); kidney-derived stem cells (KSCs).

## Graphical Abstract



This study describes the development of a novel large animal model of chronic kidney disease (CKD)-induced heart failure with preserved ejection fraction (HFpEF). Renal intra-arterial delivery of allogeneic MSCs and KSCs improved glomerular filtration rate (GFR). RNA-Seq data showed decreased podocyte apoptosis, reactive oxygen species, inflammatory pathways, and renin-angiotensin system activation. Allogeneic cell combination therapy (ACCT) restored diastolic function toward normal and decreased titin protein markers of stiffness. Cell therapy also prevented the increase in blood pressure over time.

## Significance Statement

Renal intra-arterial delivery of allogeneic mesenchymal stem cells (MSCs) and kidney-derived stem cells (KSCs) was safe and improved renal function and ameliorated diastolic dysfunction in a large animal model of chronic kidney disease (CKD)-induced heart failure with preserved ejection fraction (HFpEF). Cell therapy also prevented the increase in blood pressure over time. These findings illustrate the importance of the interaction between different populations of progenitors and the safety of allogeneic cell therapy, encouraging the further development of preclinical and clinical trials in the HFpEF and CKD populations.

## Introduction

Meaningful advances in cardiology have reduced the morbidity and mortality of ischemic heart disease and heart failure with reduced ejection fraction (HFrEF). However, there is a pressing need to develop therapeutic approaches for heart failure with preserved ejection fraction (HFpEF),<sup>1</sup> which affects ~50% of patients with heart failure,<sup>2</sup> carries a similar morbidity and mortality to HFrEF, and has a prognosis that has not improved over the last 3 decades.<sup>1,3-6</sup> HFpEF is a heterogeneous condition involving multiple comorbidities, including chronic kidney disease (CKD), metabolic syndrome, and pulmonary hypertension. Therefore, novel interventions that specifically target the pathophysiologic mechanisms underlying HFpEF are crucial to reduce its associated morbidity and mortality.

Left ventricular hypertrophy (LVH), the primary manifestation of CKD-associated cardiomyopathy, occurs in 60%-80% of patients with end-stage renal disease (ESRD) and is an independent risk factor for mortality. LVH in these patients is approximately 15 times higher than in the general population.<sup>7</sup> Interestingly, patients with kidney transplant show decreased LVH and improved cardiac function,<sup>8-10</sup> indicating that renal function is a main determinant of LVH.<sup>11,12</sup> The mechanisms underlying LVH and HFpEF in CKD patients include pressure and volume overload, anemia, “uremic” state, neurohormonal dysregulation, oxidative stress, and inflammatory state.<sup>13,14</sup> Phenotypic classification of HFpEF associated with CKD includes pathologic LV remodeling characterized by increased LV mass index and relative wall

thickness, impairment of right ventricular relaxation, increased stroke work, and impaired ventricular arterial coupling. Importantly, CKD-associated HFpEF manifests worse adverse outcomes, including hospitalization and deaths, compared to other phenotypes of HFpEF.<sup>15</sup>

In preclinical studies and clinical trials, cell-based therapy has produced encouraging results, including reduced cardiac fibrosis, decreased inflammation, and increased neovascularization, thus promoting reverse remodeling and improving cardiac structure and function in ischemic (ICM) and non-ischemic (NICM) cardiomyopathies with HFrEF.<sup>16-21</sup> Importantly, intramyocardial delivery of bone marrow-derived mesenchymal stem cells (MSCs) enhances the proliferation and differentiation of endogenous stem cells,<sup>22-24</sup> supports the stem cell niche, stabilizes the extracellular matrix, and promotes degradation of fibrotic tissue in the myocardium.<sup>25-27</sup> Allogeneic MSCs restore endothelial function in ICM and NICM patient populations as measured by flow-mediated vasodilatation and endothelial progenitor cell (EPC) colony formation.<sup>23</sup> In addition, allogeneic MSCs ameliorate chronic inflammatory responses by decreasing TNF- $\alpha$  and reversing the exhausted immune phenotype in a NICM population.<sup>18</sup>

Kidney-derived stem cells (KSCs) were initially described by Rangel et al as CD117 (c-kit<sup>+</sup>) cells present in the thick ascending limb of Henle’s loop that exhibit stem cell properties in vitro, including self-renewal capacity, clonogenicity, and multipotentiality.<sup>28,29</sup> In an acute ischemia-reperfusion rat model, these cells promoted renal recovery compared to placebo by improving proliferation of epithelial tubular

cells resulting in less tubular damage.<sup>28</sup> Further studies found that these kidney-derived cells improved podocyte foot process effacement and autophagy in an acute puromycin aminonucleoside nephropathy rat model.<sup>30</sup> Together, these beneficial cardiac and renal findings raise the question of whether allogeneic cell therapy is effective in cardiorenal syndromes, specifically CKD-associated HFpEF.

Large animal models are essential to investigate the mechanisms underlying HFpEF and to develop novel therapies prior to conducting human clinical trials. However, there are few established large animal models of HFpEF.<sup>31-33</sup> We have previously shown using an angiography-guided embolization approach to produce a 5/6 nephrectomy in a swine model, that the remnant kidney mass remaining after embolization compensates through hyperfiltration, which contributes to the development of CKD<sup>33-36</sup> and associated HFpEF.<sup>33</sup> Four weeks after embolization, swine were randomized to receive placebo, allogeneic bone marrow-derived MSCs, allogeneic KSCs, or allogeneic cell combination therapy (ACCT; MSCs + KSCs) via the renal artery of the remnant kidney. We sought to determine whether: (1) ACCT and allogeneic single-cell therapy are safe; (2) ACCT ameliorates HFpEF to a greater extent than single-cell therapy and placebo; and (3) ACCT improves renal function compared to single-cell therapy and placebo.

## Materials and Methods

All animal protocols were reviewed and approved by the University of Miami Institutional Animal Use and Care Committee. The study was conducted in a blinded fashion. One investigator, who did not conduct the experiments or analyses, was responsible for the randomization. The animal caretakers and investigators conducting the experiments, assessments, measurements, and quantification of all results were blinded to the intervention until all analyses were completed. The data were collected and processed and only when analyses were completed was the data grouped for statistical analyses by the investigator responsible for the randomization.

### CKD Induction and Stem Cell Injection

Female Yorkshire swine underwent angiographically guided, catheter-induced 5/6 nephrectomy.<sup>33</sup> One complete kidney and 2/3 of the other underwent polyvinyl alcohol (PVA) particle<sup>33,34,37</sup> and ethanol infusion<sup>33</sup> into the renal arteries to create a CKD model (Supplementary Fig. 1). Four weeks after embolization, 26 animals were randomized to receive delivery of either: allogeneic bone marrow-derived MSCs ( $n = 6$ ,  $1 \times 10^7$ ), allogeneic KSCs ( $n = 6$ ,  $1 \times 10^7$ ), ACCT (MSCs + KSCs;  $n = 7$ , 1:1 ratio [total =  $1 \times 10^7$  cells]), or placebo ( $n = 7$ , Plasma-Lyte, Baxter, IL, USA) via the patent renal artery of the remnant kidney (Supplementary Fig. 2).

### Cell Manufacturing and Delivery

KSCs were isolated from cortical and medullary kidney biopsies from 2 male Yorkshire Swine using magnetic selection for CD117 (c-kit). After magnetic selection, KSCs were expanded, characterized by flow cytometry, and cryopreserved after the third passage (see Supplementary Methods). MSCs were manufactured from bone marrow aspirates collected from the femur of the same 2 swine donors. Upon collection of bone marrow aspirates, the product was centrifuged on top of lymphocyte separation media (Ficol Hypaque) and processed to obtain MSCs

as previously described<sup>22,24,38-40</sup> (see Supplementary Methods). Cell characterization was performed by flow cytometry before cryopreservation and after third passage. On the day of injection, cells were thawed and tested to determine viability ( $\geq 70\%$ ), sterility for STAT gram stain (negative), mycoplasma (negative), and endotoxins ( $< 5$  EU/mL). Injectate (placebo or re-suspended cells) was divided into 10 syringes of 0.5 mL each and administered slowly into the different patent segmental arteries to cover all the remnant parenchyma. Cell therapy or placebo delivery was performed at 4-week post-embolization using a soft tip cobra catheter (4-5 Fr Johnson & Johnson, New Brunswick, NJ, USA) into the patent 1/6 kidney, guided by contours of an angiogram and MRI.

### Study Endpoints

Each animal underwent extensive safety evaluation of allogeneic cell delivery including mixed lymphocyte reaction (MLR), macroscopic evaluation at necropsy, and histologic evaluation of liver, spleen, heart, kidney, lung, and ileum by a specialized pathologist for evaluation of neoplastic tumor formation and signs of acute or chronic rejection. Kidney functional, structural, and molecular measurements for validation of the CKD model and evaluation after cell treatment included: glomerular filtration rate (GFR) measurement using inulin, anatomical and perfusion evaluation by renal MRI (3.0T clinical scanner, Magnetom, Siemens AG, Munich, Germany), laboratory measurements, including serum creatinine and blood urea nitrogen (BUN), protein and creatinine in urine, hematology, and chemistry, histology, and RNA-Seq analyses (see Supplementary Methods). In addition, to evaluate HFpEF characteristics, we used cardiac MRI to assess cardiac function and morphology, including cardiac volumes, LV ejection fraction (EF), wall thickness, chamber diameters, and Eulerian circumferential strain. Pressure-volume (PV) Loops (Millar Instruments Inc., Houston, TX, USA) were used to evaluate end-diastolic pressure (EDP), end-diastolic pressure-volume relationship (EDPVR), end-systolic pressure (ESP), and end-systolic pressure-volume relationship (ESPVR). We also performed cardiac histology and tissue analysis for fibrosis, cardiomyocyte area, capillary density, and titin phosphorylation (see Supplementary Methods).

### Statistics

Data distribution, for continuous measures, was assessed using the Pearson normality test. Continuous variables non-normally distributed were examined by Mann-Whitney *U* test and described by median and interquartile range (IQR). Normally distributed variables were evaluated by two-way ANOVA and multiple comparisons were estimated using the Bonferroni and Tukey corrections and expressed as mean  $\pm$  SE. Within data, normally distributed were analyzed by paired *t* test, otherwise by Wilcoxon matched-pairs test. Categorical variables were evaluated by the Pearson's chi-squared test and Fisher's exact test as corresponding. Imputation was not performed for missing data. All statistics were tested using two-sided at  $\alpha = 0.05$ . Analyses were done using GraphPad Prism7 (GraphPad Software, Inc. La Jolla, CA, USA).

## Results

The renal embolization was performed in female Yorkshire swine (30-35 kg). This procedure to create a remnant kidney model of CKD carries a high mortality rate, as previously

described by Misra et al and our group.<sup>33,34</sup> Seventeen animals died before cell therapy administration, the majority within the first week, as expected, from which: 1 was euthanized after lower limb paralysis, 1 had a complication after anesthesia, and 15 died as a complication of acute kidney injury within the first week after embolization. Twenty-six animals successfully completed the study and were included in this analysis. Follow-up evaluations were done weekly until cell therapy or placebo delivery at 4-week post-embolization. Animals were studied for a total of 12 weeks post-embolization (8 weeks post-cell therapy or placebo delivery) (Supplementary Fig. 2).

### Development of CKD After Embolization

The CKD model was confirmed by an increase in creatinine from baseline ( $1.25 \pm 0.04$  mg/dL) to 4-week post-embolization ( $2.37 \pm 0.1$  mg/dL; 95% CI: 0.85 to 1.40,  $n = 26$ ;  $P < .0001$ ; Fig. 1A), increase in BUN from 9 mg/dL (8, 11) to 23.5 mg/dL (18.7, 30,  $n = 26$ ;  $P < .0001$ ; Fig. 1B), and decrease in GFR from  $111.4 \pm 6.4$  mL/minute to  $46.03 \pm 4.58$  mL/minute (95% CI: -79.31 to -48.51,  $n = 26$ ;  $P < .0001$ ; Fig. 1C). Similarly, renal perfusion decreased from baseline ( $130.1 \pm 7.3$  ROI) to 4-week post-embolization ( $91.4 \pm 8.8$  ROI [95% CI: -55.73 to -21.75];  $P < .0001$ ; Fig. 1D). However, the protein/creatinine ratio did not change between baseline (0.38 [0.18, 0.58]) and 4 weeks post-embolization (0.59 [0.38, 0.82];  $P = .42$ ; Fig. 1E). Similarly, mean arterial pressure (MAP) was not different between baseline ( $48.32 \pm 2.08$  mmHg) and 4 weeks post-embolization ( $46.19 \pm 1.92$  mmHg [95% CI: -7.23 to 2.98];  $P = .4$ ; Fig. 1F).

### Manifestations of CKD-Induced HFpEF in a Swine Model

LVH was evidenced by an increase in left ventricular end-diastolic (LVED) mass to body surface area (BSA) ratio

from baseline ( $72.69 \pm 2.47$  g) to 4 weeks post-embolization ( $81.38 \pm 2.91$  g [95% CI: 4.8 to 12.57],  $n = 26$ ;  $P < .0001$ ; Fig. 2A) and increased relative wall thickness from  $0.26 \pm 0.01$  to  $0.31 \pm 0.01$  mm (95% CI: 0.03 to 0.07,  $n = 26$ ;  $P < .0001$ ; Fig. 2B).

LV diastolic function was evaluated by PV loops. EDP was significantly increased from baseline ( $10.6 \pm 0.87$  mmHg) to 4 weeks post-embolization ( $13.23 \pm 1.12$  mmHg [95% CI: 0.07 to 5.14],  $n = 13$ ;  $P = .045$ ; Fig. 2C). Similarly, EDPVR increased from baseline (0.19 [0.14, 0.24]) to 4 weeks post-embolization (0.31 [0.23, 0.38],  $n = 13$ ;  $P = .0002$ ; Fig. 2D). Finally, isovolumetric relaxation measured by  $dP/dt_{\min}$  was reduced after 4 weeks post-embolization by  $-229.7 \pm 96.08$  (95% CI: -437.3 to -22.12,  $n = 13$ ;  $P = .03$ ).

Systolic function was preserved during the study, as evidenced by maintenance over time of EF and stroke volume (SV) (Table 1). Contractility evaluated by ESPVR increased from baseline ( $0.79 \pm 0.08$ ) to 4 weeks post-embolization ( $1.13 \pm 0.11$  [95% CI: 0.15 to 0.52],  $n = 13$ ;  $P = .0017$ ). Tagged harmonic phase cardiac magnetic resonance strain maps demonstrated a maintained LV peak Eulerian circumferential shortening strain (Ecc) from baseline to 4 weeks post-embolization.

### Characterization of Allogeneic MSCs and KSCs

Swine MSCs used for cell therapy were characterized by flow cytometry, as previously described.<sup>22,24,38-40</sup> The MSCs expressed CD105 and CD90 but not CD45 (Supplementary Fig. 3). KSC characterization<sup>28</sup> by flow cytometry showed expression of CD117, CD90, and CD133 but not CD45 (Supplementary Fig. 4).

### Safety of Allogeneic Cell Single and Combination Therapy

After intra-arterial cell delivery at 4 weeks post-embolization, animals were followed for 8 weeks post-cell/placebo delivery

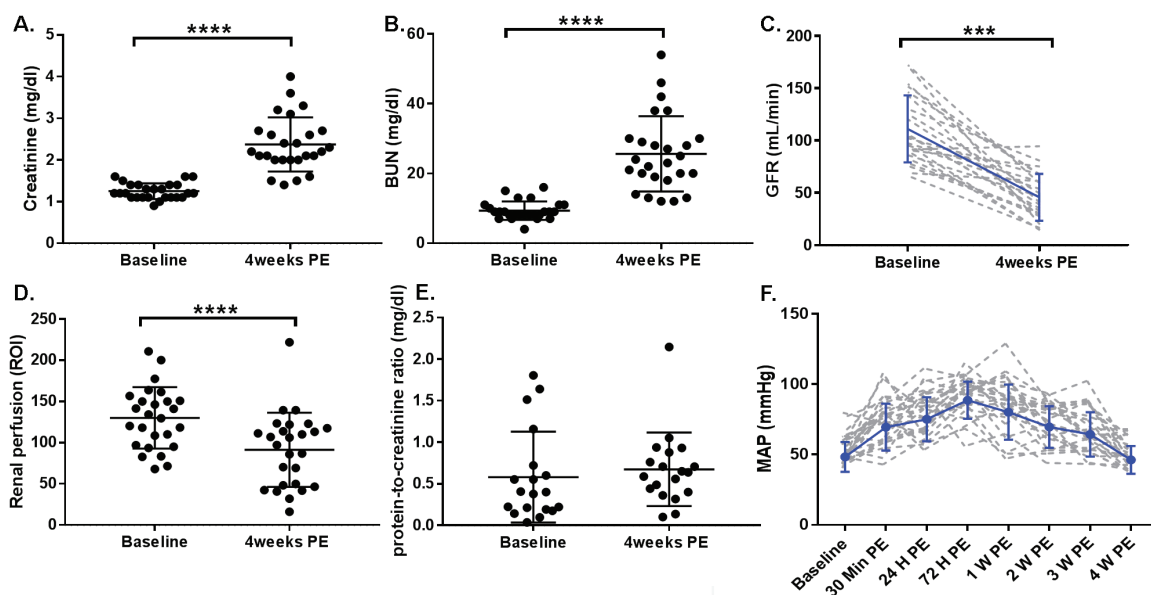


**Figure 1.** Development of chronic kidney disease (CKD) after embolization. The CKD model was validated from baseline ( $N = 26$ ) to 4 weeks by an increased (A) creatinine ( $P < .0001$ ) and (B) blood urea nitrogen (BUN,  $P < .0001$ ) and decreased (C) glomerular filtration rate (GFR) ( $P < .0001$ ) and (D) renal perfusion ( $P < .0001$ ). (E) Urine protein/creatinine ratio and (F) mean arterial pressure (MAP) did not change over time.



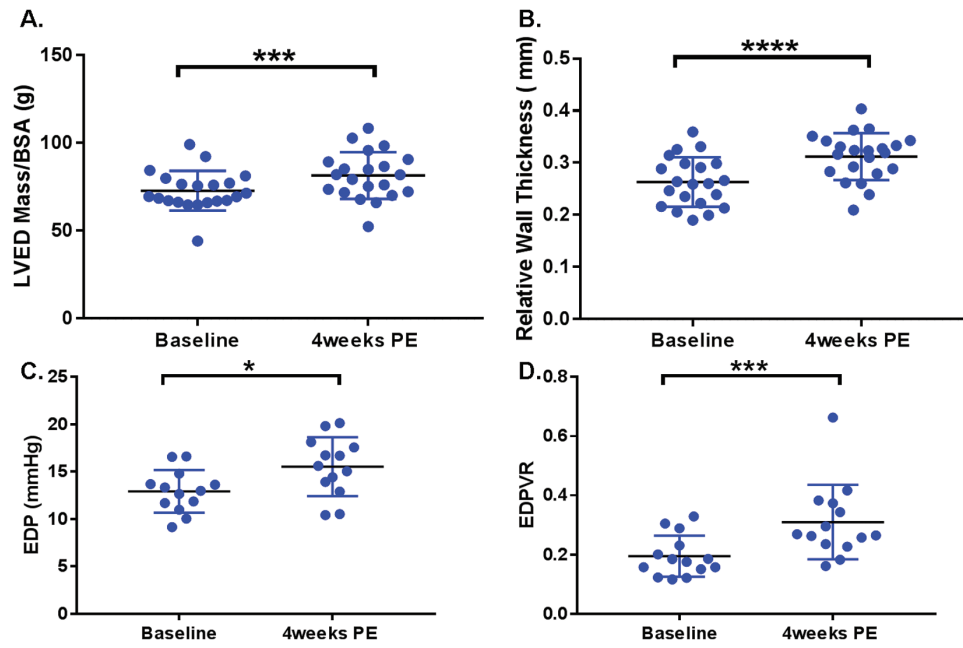


**Figure 2.** Signs of CKD-induced heart failure with preserved ejection fraction (HFpEF). HFpEF was demonstrated at 4 weeks by increases in (A) left ventricular (LV) mass ( $P < .0001$ ), (B) relative wall thickness ( $P < .0001$ ) as evaluated by MRI ( $N = 26$ ), (C) end-diastolic pressure (EDP;  $P = .045$ ), and (D) end-diastolic pressure-volume relationship (EDPVR;  $P = .0002$ ) as evaluated by pressure-volume (PV) loops ( $N = 13$ ).

and found to have no signs of hyper-acute, acute, or chronic allergic reaction. Histologic evaluation of the remnant kidney and the heart was performed by 2 different pathologists that were blinded to treatment. No signs of lymphocytic infiltration or necrosis within the tissue were reported. MLR assays did not show any acute immune response compared to phytohemagglutinin (PHA) (the 26 animals were included in MLR assays) (Fig. 3A). No ectopic tissue formation, remote areas of inflammation, or tumors were observed in any group by necropsy or histology. In a subgroup of animals ( $n = 4$ ), cells were labeled with iron nanoparticles and tracked by MRI immediately, 30 minutes, 24 hours, and 1 week after delivery. A concentration of the cells was present in the cortex area of the patent kidney (Fig. 3B). The distribution of the product was not different between the groups.

### Renal Functional Improvement in Response to Allogeneic Cell-Based Therapy

At 12 weeks post-embolization, the MAP showed significant difference between the groups (delta between groups;  $P = .031$ ), with an increase predominantly in the placebo group ( $\Delta 21.89 \pm 6.05$  mmHg; 95% CI:  $-32.25$  to  $-10.19$ ;  $P < .0001$ ; Fig. 4A). This increase was significant compared to the ACCT group, which maintained stable MAP over time after the 4-week post-embolization time point ( $\Delta 2.42 \pm 2.86$ ; 95% CI:  $-14.33$  to  $9.494$ ,  $n = 6-7$ ;  $P = .94$ ; two-way ANOVA 0.006, multiple comparison ACCT vs. Placebo,  $P = .04$ ; Fig. 4A). Also, MSC- and KSC-treated groups exhibited no change in MAP over time from 4-week post-embolization to 12-week post-embolization (end of the study). Kidney function, directly measured by GFR, improved only in the ACCT group by  $67.21 \pm 21.35$  mL/minute (95% CI:  $-112.9$  to  $-21.5$ ,  $n = 6$ ;  $P = .002$ ) from 4- to 12-week post-embolization (Fig. 4B). Other parameters such as BUN, creatinine, urine protein to creatinine ratio (Fig. 4C), total kidney volume (Fig. 4D), and kidney perfusion did not change for any group from 4-week

post-embolization to the end of the study (Table 1). Total kidney mass was similar between the groups at 12 weeks post-embolization.

Histologic analyses revealed mild global sclerosis and segmental sclerosis in the remnant kidneys of all the treatment groups. Interstitial fibrosis and inflammation, subcapsular region edema, tubular injury, vascular calcification, and arteriosclerosis were similarly mild in all treatment groups (Supplementary Fig. 5). Glomerular area was increased in the placebo-treated group, which, together with the functional data, suggests that even with greater hypertrophy the placebo group was not able to compensate for the reduced functional capacity compared to the cell-treated groups (Fig. 4E).

Differential expression analysis by RNA-Seq revealed a significant ( $P < .05$ ) decrease in 1645 genes and an increase in 206 genes in the kidneys of the ACCT-treated groups compared to placebo (Fig. 5A). Gene set enrichment analysis (GSEA) showed a significant decrease in multiple pathways. Of the top 10 significantly downregulated and upregulated pathways, there were decreases in genes normally increased in kidney transplant rejection ( $q < 10^{-6}$ , NES =  $-2.32$ ) and in genes involved in extracellular matrix disassembly ( $q < 10^{-6}$ , NES =  $-2.20$ ), and an increase in oxidative respiration ( $q < 10^{-6}$ , NES =  $3.45$ ) (Fig. 5B). Complementary to our GSEA results, ingenuity pathway analysis (IPA) of the placebo and the combination group showed that ACCT administration downregulated genes related to oxidative stress (fold change =  $-4.6$ ,  $P < .0001$ ), fibrosis, inflammatory response (fold change =  $-4.760$ ,  $P < .05$ ), and apoptosis of various kidney cell types (fold change =  $-24.89$ ,  $P = .004$ ) (Fig. 5C), including podocytes (fold change =  $-2.065$ ,  $P = .04$ ) and mesangial cells proliferation (fold change =  $-2.530$ ,  $P < .05$ ). Consistent with these results, there was a downregulation of canonical drivers of tubular damage and regeneration including SOX9 (fold change =  $-2.39$ ,  $P = .0004$ ) and TGF- $\beta$  (fold change =  $-1.69$ ,  $P = .006$ ) after ACCT treatment. Exploring

**Table 1.** Laboratory parameters at baseline, 4-week post-embolization, and 12-week post-embolization.

Group parameter	Baseline			4-wk post-embolization			12-wk post-embolization			Two-way ANOVA P value			
	Placebo	MSC	KSC	ACCT	Placebo	MSC	KSC	ACCT	Placebo		MSC	KSC	ACCT
<b>Renal function</b>													
MAP (mmHg)	46.26 ± 4.65	47.89 ± 3.44	52.64 ± 5.31	46.89 ± 3.75	44.89 ± 3.92	45.22 ± 3.75	44.83 ± 4.73	50.22 ± 3.56	66.11 ± 5.82****	50.98 ± 3.36	46.46 ± 2.63	52.64 ± 3.60	.006
GFR	97.02 ± 3.35	124.00 ± 13.27	115.90 ± 12.24	106.70 ± 18.03	41.50 ± 7.48	51.61 ± 8.34	47.23 ± 13.24	43.77 ± 8.55	74.94 ± 15.88	81.83 ± 25.48	76.14 ± 13.00	111.00 ± 23.97**	.48
Creatinine (mg/dL)	1.29 ± 0.07	1.17 ± 0.09	1.30 ± 0.08	1.25 ± 0.06	2.60 ± 0.27	1.97 ± 0.14	2.58 ± 0.27	2.37 ± 0.30	2.49 ± 0.30	2.27 ± 0.18	2.82 ± 0.17	2.33 ± 0.29	.53
BUN (mg/dL)	11.00 ± 8.00	8.00 ± 7.18	8.50 ± 7.00	10.00 ± 8.00	30.00 ± 13.81	21.14 ± 4.91	26.17 ± 10.59	25.17 ± 12.62	23.00 ± 3.44	19.86 ± 2.06	21.83 ± 2.37	20.50 ± 4.75	.66
Creatinine/urine protein	0.31 ± 0.07	0.80 ± 0.39	0.32 ± 0.12	0.30 ± 0.13	0.56 ± 0.12	0.69 ± 0.18	0.54 ± 0.17	1.06 ± 0.55	0.50 ± 0.11	0.46 ± 0.03	0.29 ± 0.05	0.56 ± 0.16	.34
<b>Cardiac function</b>													
EF (%)	39.91 ± 2.13	41.72 ± 2.79	41.26 ± 0.96	38.25 ± 3.53	42.88 ± 2.66	45.71 ± 6.94	43.25 ± 3.24	41.95 ± 5.05	47.41 ± 1.25	48.24 ± 3.67	45.45 ± 1.22	48.48 ± 3.41	.64
EDV/BSA (mL)	121.10 ± 14.15	115.70 ± 8.26	121.30 ± 11.72	116.40 ± 6.54	111.20 ± 8.63	106.30 ± 4.73	115.50 ± 13.56	111.80 ± 4.41	109.60 ± 8.06	101.80 ± 8.16	106.30 ± 9.99	109.70 ± 5.91	.89
ESV/BSA (mL)	69.68 ± 7.48	93.21 ± 8.43	71.37 ± 7.29	72.76 ± 8.09	61.94 ± 5.02	87.66 ± 9.06	65.09 ± 6.82	65.18 ± 4.70	57.23 ± 5.20	77.90 ± 10.70	58.49 ± 6.38	56.52 ± 4.66	.90
SV/BSA (mL)	45.98 ± 4.68	85.19 ± 12.75	49.91 ± 4.70	43.65 ± 2.05	46.11 ± 2.20	79.47 ± 13.55	50.40 ± 7.04	46.58 ± 1.56	51.36 ± 2.82	79.58 ± 10.16	47.85 ± 3.77	53.14 ± 4.40	.21
Relative wall thickness	0.26 ± 0.02	0.26 ± 0.03	0.28 ± 0.02	0.25 ± 0.02	0.30 ± 0.02	0.31 ± 0.02	0.31 ± 0.02	0.33 ± 0.02	0.30 ± 0.01	0.36 ± 0.04	0.35 ± 0.02	0.35 ± 0.01	.494
dP/dt <sub>max</sub>	802.30 ± 106.90	784.00 ± 273.30	746.10 ± 73.87	616.50 ± 140.80	907.10 ± 106.30	1156.00 ± 135.00	999.00 ± 84.90	868.50 ± 175.40	1250.00 ± 307.40	1149.00 ± 124.50	1536.00 ± 849.70	998.30 ± 114.70	.623
ESPVR	0.80 ± 0.51	0.88 ± 0.15	0.68 ± 0.42	0.78 ± 0.18	1.06 ± 0.58	1.12 ± 0.39	1.06 ± 0.24	1.24 ± 0.60	0.75 ± 0.16	0.90 ± 0.33	1.06 ± 0.21	0.58 ± 0.05	.719

Note: This table shows the establishment of the CKD-induced HFpEF model prior to treatment at 4 weeks and after 8 weeks of treatment.

\*\* $P = .01$  and \*\*\* $P < .0001$  compared with 4-week post-embolization. Two-way ANOVA  $P$  values refer to analysis within groups throughout the model establishment, paired  $t$  test. No difference between groups at 4-week post-embolization time point. All data are expressed as mean ± SEM.

Abbreviations: ACCT, allogeneic combination cell therapy; BUN, blood urea nitrogen; EDV/BSA, end-diastolic volume corrected by body surface area; EF, ejection fraction; ESPVR, end-systolic pressure-volume relationship; ESV/BSA, end-systolic volume corrected by body surface area; GFR, glomerular filtration rate; KSC, kidney-derived stem cell; MAP, mean arterial pressure; MSC, mesenchymal stem cell; SV, stroke volume.

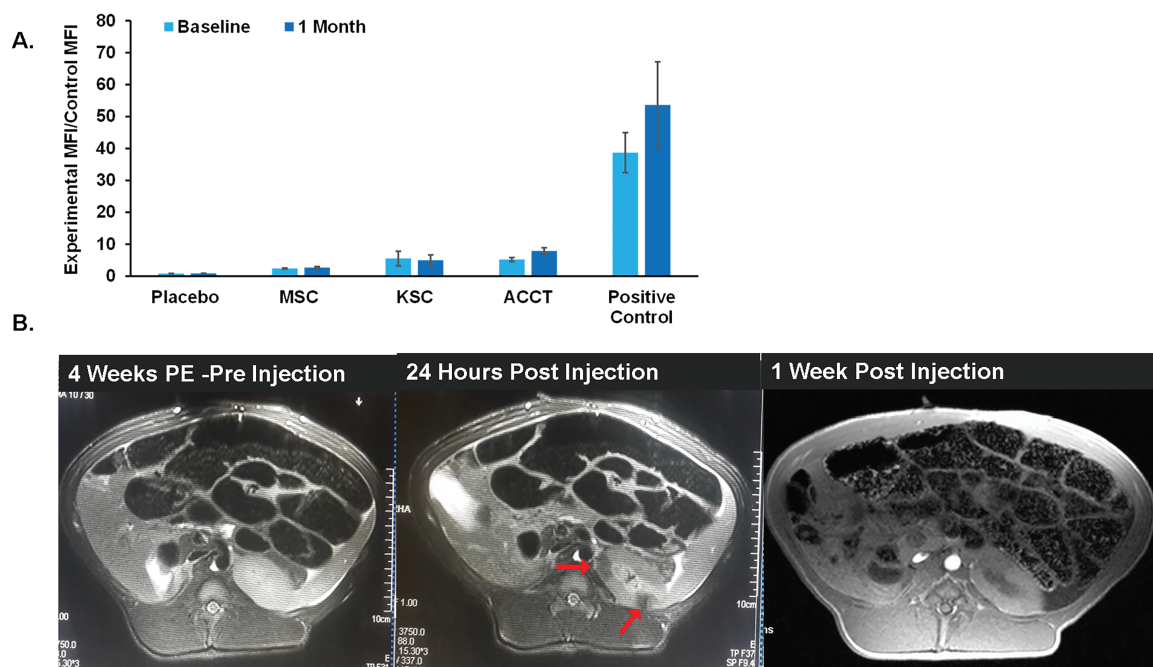


**Figure 3.** Safety of allogeneic cell single and combination therapy. The absence of immune response to allogeneic cell therapy. (A) Allogeneic MSCs, KSCs, or combination cell therapy did not elicit an acute immune response, evaluated by mixed lymphocyte reaction ( $n = 26$ ). Positive control used was phytohemagglutinin (PHA). (B) Evidence of cell localization in the cortex of the remnant kidney 24 hours after cell delivery.

this further, subpathway IPA revealed that the ACCT group manifested downregulated renin-angiotensin signaling (fold change =  $-3.162$ ,  $P = .024$ ; angiotensinogen; fold change =  $-5.332$ ) (Fig. 5D), endothelin-1 signaling, pro-inflammatory cytokines, WNT, and FGF-2, all of which are related to cardiac hypertrophy (cardiac hypertrophy signaling canonical pathway; fold change =  $-7.23$ ,  $P < .0001$ ).

### Combination Cell-Based Therapy Restores Diastolic Function

We examined cardiac function after cell delivery. EF remained stable over time in all groups. LVED mass corrected by body weight (Fig. 6A) and relative wall thickness (Table 1) was stable from 4- to 12-week post-embolization, with no difference between the groups. Diastolic evaluation revealed stable EDP in all groups from 4- to 12-week post-embolization (Fig. 6B). However, the ACCT group showed improvement in passive diastolic function as shown by the decrease of EDPVR from 4 weeks to 12 weeks ( $\Delta 0.23 \pm 0.13$ ; 95% CI: 0.078 to 0.386;  $n = 3$ ;  $P = .003$ ; Fig. 6C). Contractility evaluated by ESPVR and  $dp/dt_{max}$  was preserved over time with no change between groups (Table 1).

### Titin Isoform Phosphorylation

There was an increase in the N2BA/N2B phosphorylation/total protein ratio, indicating a “stiff” N2B titin isoform in the placebo group compared to a normal control not embolized ( $n = 3$ ;  $P \leq .0001$ ; Fig. 6D and Supplementary Fig. 6). The MSC-treated group had the lowest ratio compared to control ( $n = 3$ ;  $P = .023$ ) with the MSC group exhibiting a reduction compared to the placebo group ( $n = 3$ ;  $P = .012$ ; Fig. 6D and Supplementary Fig. 6). These results are consistent with the increase in EDP and EDPVR in the placebo group, indicating cardiac muscle stiffening and decreased relaxation characteristic of diastolic dysfunction.

### Fibrosis, Capillary Density, and Cardiomyocyte Evaluation

Intra myocardial and perivascular fibrosis and collagen deposition evaluated by trichrome staining and picosirius red, respectively, was mild in the left atrium and left ventricle, and similar between the groups (Supplementary Fig. 7). Collagen III, as quantified by Western blot, showed a trend toward increasing in the placebo group; however, no statistically significant change was seen compared to control or any other group (Supplementary Fig. 7).

Cardiomyocyte hypertrophy, as evaluated by cardiomyocyte area measurement, did not show any difference between the groups (Fig. 6E). Capillary density showed a trend toward higher density in the ACCT and lower density in the placebo group, however, there was no statistically significant difference between the groups (Fig. 6F).

### Discussion

This blinded, placebo-controlled, preclinical study tested the safety and effectiveness of ACCT compared to single-cell therapy on renal and cardiac functional parameters in a large animal model of CKD-induced HFpEF we developed.<sup>33</sup> The results support the feasibility of a large animal model of CKD due to nephron loss, which develops characteristic structural and functional signs of HFpEF, including increases in relative LV wall thickness, EDP, and EDPVR and modification in titin phosphorylation. Furthermore, we demonstrate that delivery of allogeneic MSCs and KSCs is safe as single-cell or combination therapy, as shown by the lack of an immune response by histologic analyses and MLR assays. Moreover, ACCT improved kidney function (GFR) and ameliorated cardiac diastolic function compared to single-cell therapy and to placebo. Combination and single-cell therapy had a beneficial effect on blood pressure compared to placebo.

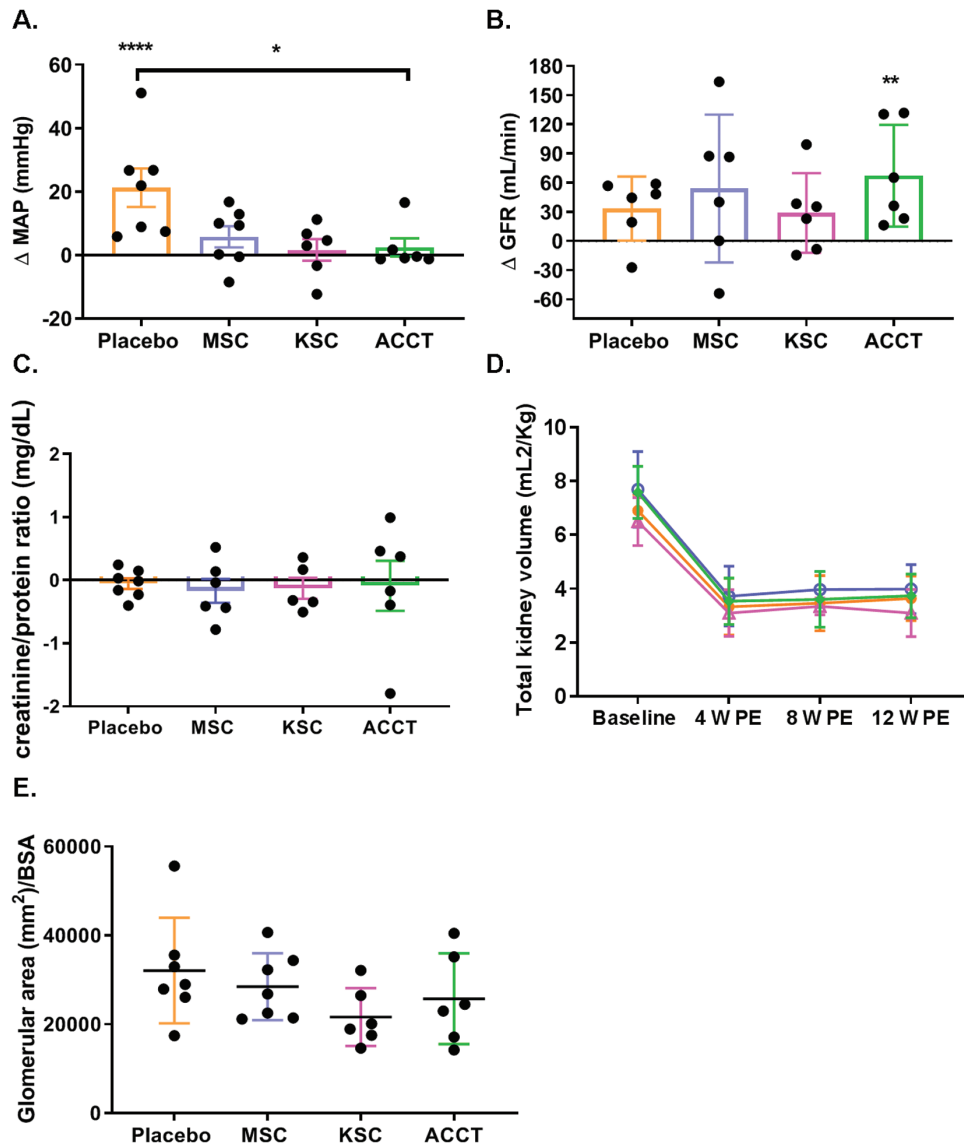


**Figure 4.** Renal functional improvement in response to allogeneic cell single and combination therapy. Improvement in blood pressure and kidney function. (A) There was a significant difference in MAP between groups ( $P = .04$ ), with an increase in the placebo group ( $P < .0001$ ). (B) GFR had the greatest improvement in the combination group ( $P = .002$ ). (C) Urine protein/creatinine ratio and (D) total kidney volumes did not change significantly in any group after cell delivery. (E) Glomerular area in the placebo group was higher, albeit not significantly, than other groups without compensation of renal function. Abbreviations: MSC, allogeneic mesenchymal stem cells; KSC, allogeneic kidney-derived stem cells; ACCT (MSCs + KSCs), allogeneic cell combination therapy.

Although our animal model manifested CKD, as demonstrated by decreased GFR, this effect was not associated with the development of hypertension at 4 weeks post-embolization. Similar results were shown by Zakeri et al in an experimental hypertensive renal wrapping canine model, which at 4 weeks had decreased blood pressure, but further follow-up at 7 weeks demonstrated an increase in blood pressure,<sup>41</sup> comparable to our placebo group at the final 12-week post-embolization time point. In our study, despite the absence of hypertension at 4 weeks post-embolization, extracellular structural changes were demonstrated by mild collagen deposition in the atria and left ventricle. Moreover, as reported in patients with HFpEF,<sup>42</sup> the placebo group exhibited alterations in titin phosphorylation, in agreement with previous investigations, including a higher phospho-N2BA/phospho-N2B ratio, secondary to a relative hypophosphorylation of the N2B titin isoform, which is related to increased

stiffness.<sup>43</sup> These cellular and molecular changes are associated with increases in left ventricular end diastolic pressure, a leftward shift in the EDPVR, and increases in relative wall thickness and LV mass.

HFpEF is a complex disease process with limited treatment options that include symptomatic treatment with diuretics.<sup>44</sup> Multiple approaches are under investigation to manage the LV diastolic dysfunction and increased left atrial pressure, volume overload, pulmonary and right ventricular dysfunction, and decipher the underlying mechanisms, including cellular and extracellular changes, cardio-metabolic abnormalities, and microvascular inflammation.<sup>6,45</sup> Translating therapies that improve HFpEF have, to date, been unsuccessful in similarly treating HFpEF.<sup>46</sup> In preclinical and clinical studies of ICM and NICM, cell therapy exerts beneficial effects on several of the pathophysiologic factors also underlying HFpEF, including extracellular matrix



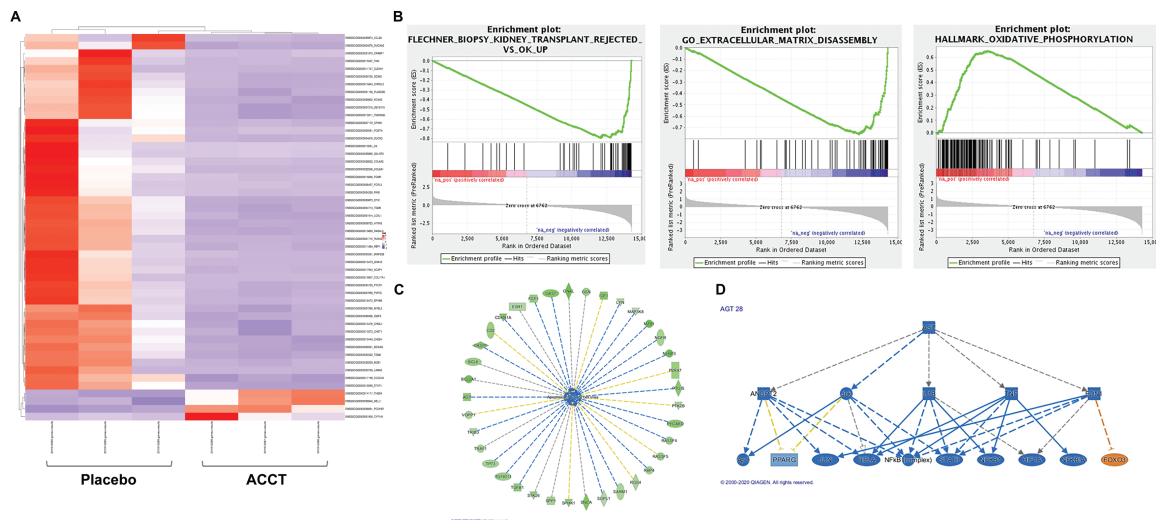


**Figure 5.** RNA data showing decreased inflammatory markers, oxidative stress, and renin-angiotensin signaling system in allogeneic cell combination therapy (ACCT) compared to placebo. RNA-Seq analysis: (A) Heat map showing the top 50 differentially expressed genes between placebo, to the left, and ACCT groups, to the right. (B) Pathways involving extracellular matrix disassembly ( $q < 10^{-6}$ , NES =  $-2.20$ ) and an increase in oxidative respiration ( $q < 10^{-6}$ , NES =  $3.45$ ) are downregulated in the ACCT group compared to placebo. (C) Kidney RNA-Seq analysis of the placebo and combination groups showed that ACCT downregulated genes related to podocyte apoptosis. Importantly, the ACCT group downregulated renin-angiotensin signaling ( $P = .024$ ) related to blood pressure and cardiac hypertrophy (D).

remodeling,<sup>47</sup> inflammatory response,<sup>18</sup> endothelial dysfunction,<sup>23</sup> and mitochondria energetics.<sup>48,49</sup> Our findings suggest that cell-based therapy may be a promising therapeutic for both HF<sub>r</sub>EF and HF<sub>p</sub>EF.

This is the first preclinical study, to our knowledge, to investigate the efficacy of combination allogeneic KSCs and MSCs in a large animal model of CKD-induced HF<sub>p</sub>EF. Several studies, including clinical trials, have evaluated the safety and efficacy of allogeneic MSC delivery in ICM and NICM, demonstrating a reduction in fibrosis and improvement in cardiac function.<sup>18,19,47</sup> The mechanisms of action underlying the effects of MSCs include niche cell-to-cell contact, stimulation of endogenous progenitors, and secretion of various paracrine mediators, such as anti-inflammatory, immunomodulatory, antifibrotic, proangiogenic, and other growth factors that promote ventricular reverse remodeling.<sup>50</sup> Our group showed that in a large animal model of ICM, the combination of allogeneic MSCs and cardiac progenitor cells was safe and lead to meaningful increases in cardiac volumes, perfusion, and cardiomyocyte mitosis compared to single-cell therapy or placebo.<sup>17</sup> The process that boosts the repair mechanisms by these 2 cell types include cardiac progenitor migration and proliferation via the SDF1/CXCR4 and stem cell factor/*c-kit* pathways.<sup>44</sup> Likewise, our previous study in an acute ischemia-reperfusion injury in rats demonstrated that KSCs and MSCs, each as single therapy, decreased the kidney injury score, tubular necrosis, brush-border loss, and tubular dilatation in comparison with placebo.<sup>28</sup> KSCs upregulate the mTOR-Rictor pathway and modulate autophagy leading to the preservation of podocytes.<sup>29,51</sup> We hypothesize that the interaction between KSCs and MSCs, perhaps via SDF1/CXCR4, promotes kidney repair mechanisms like that observed in the heart. However, this mechanism requires further study.<sup>52</sup>

It was recently proposed that microvascular coronary dysfunction, which is associated with decreased GFR,<sup>53</sup> and increased uremic toxins,<sup>54</sup> systemic inflammation,<sup>55</sup> and oxidative

stress,<sup>56</sup> is a common denominator in the main comorbidities affecting HF<sub>p</sub>EF.<sup>56</sup> The injured renal parenchyma releases TNF- $\alpha$ , IFN- $\gamma$ , monocyte chemoattractant protein (MCP-1), and interleukin (IL)-10, which may lead to myocardial injury.<sup>57</sup> Mechanisms underlying microvascular coronary dysfunction include reduced nitric oxide availability and increased formation of peroxynitrite in the adjacent endothelium.<sup>56</sup> Our RNA-Seq analyses support the notion that ACCT modulates oxidative stress and exerts an anti-apoptotic and immunomodulatory effect in the kidney. Furthermore, ACCT downregulated HIF-1 $\alpha$ , TGF- $\beta$ , and NF- $\kappa$ B, which are related pro-fibrotic signaling pathways implicated in CKD,<sup>58,59</sup> as well as decreased renin-angiotensin system activation. Together, these effects may have contributed to the improved kidney function. In contrast, the greater glomerular hypertrophy secondary to hyperfiltration in the placebo-treated group did not improve kidney function or reduce blood pressure. Consistent with these results, treatments that decrease glomerular hyperfiltration, such as inhibitors of the renin-angiotensin-aldosterone system slow progression of CKD.<sup>60</sup>

Saad et al<sup>61</sup> assessed the safety and efficacy of intra-arterial infusion of autologous adipose tissue-derived MSCs into the post-stenotic renal artery versus standard therapy only in patients with renovascular disease (without revascularization). They demonstrated reduced renal tissue hypoxia in the post-stenotic kidney and increased cortical perfusion and renal blood flow (RBF) in the post-stenotic and the contralateral kidneys. Single-kidney GFR remained stable after MSC treatment but fell in the standard therapy-only group. These findings are consistent with those in the present study. Moreover, a recent phase I study in patients with atherosclerotic renovascular disease showed that renal arterial infusion of autologous MSCs decreased inflammatory markers and improved GFR, blood pressure, RBF, and hypoxia 3 months after infusion.<sup>62</sup>

There is also evidence that cellular and extracellular structural changes in HF<sub>p</sub>EF are mediated via the activation of

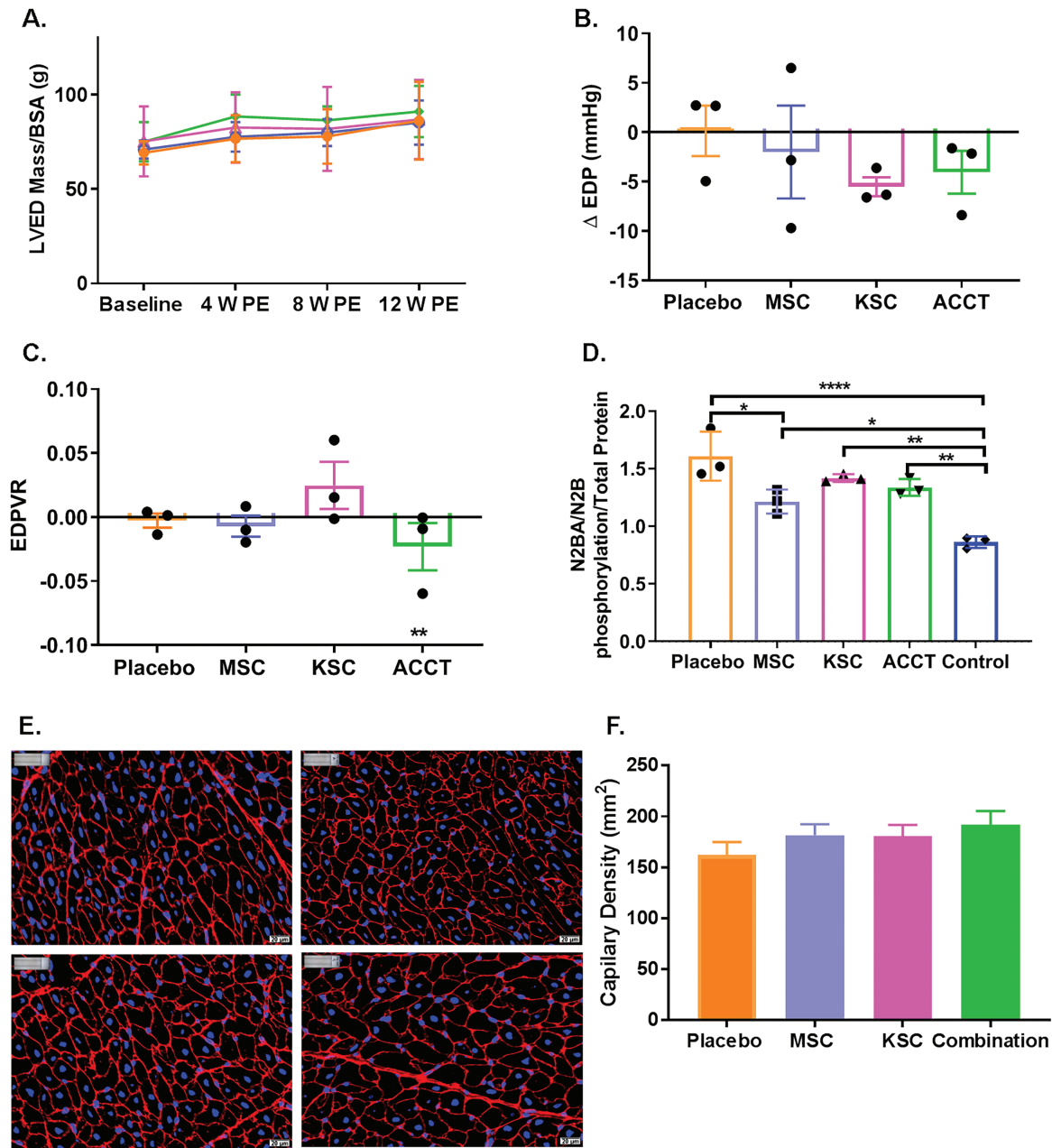


**Figure 6.** Allogeneic cell combination therapy (ACCT) restores diastolic dysfunction. Improvement in diastolic dysfunction. (A) Left ventricular end-diastolic (LVED) mass and (B) end-diastolic pressure (EDP) did not change significantly at 12 weeks. However, (C) ACCT improved EDPVR significantly ( $\Delta$ EDPVR;  $P = .003$ ). (D) Molecular analyses demonstrated the changes in titin phosphorylation in the placebo- compared to the MSC-treated group. (E) Cardiomyocyte area did not differ between groups. Cardiomyocytes ( $n = 50$  per sample) were evaluated by WGA rhodamine immunofluorescent staining ( $n = 5$  per group). (F) Capillary density showed a trend toward higher capillary density in the ACCT group; however, there was no significant difference between groups. Three random areas were evaluated by Alexa Fluor 488 isolectin immunofluorescent staining ( $N = 5$  per group). Abbreviations: MSC, allogeneic mesenchymal stem cells; KSC, allogeneic kidney-derived stem cells; ACCT (MSCs + KSCs), allogeneic cell combination therapy.

the renin-angiotensin-aldosterone system. Angiotensin II is associated with upregulation of TGF- $\beta$  in myofibroblasts and cardiomyocytes that suppresses matrix metalloproteinases (MMPs) thus causing net extracellular matrix buildup in the interstitial space,<sup>63,64</sup> which in addition to cardiomyocyte hypertrophy, ultimately leads to diastolic dysfunction.<sup>1,65</sup> Importantly, ACCT downregulated the renin-angiotensin system,<sup>60,66</sup> endothelin-1 signaling,<sup>62</sup> pro-inflammatory cytokines, WNT, TGF- $\beta$ ,<sup>67</sup> and FGF-2, and could play a primary role in the improvement of cardiac diastolic function in the

ACCT group. Although EDP over time did not significantly decrease, its downward trend correlates with the significant decrease of EDPVR in the ACCT group. This improvement in the relationship between cardiac and renal function was evident initially in patients with ESRD after kidney transplantation, who manifested a reversal of cardiac remodeling patterns.<sup>68</sup> Similarly, in a non-atherosclerotic renovascular hypertensive porcine model, percutaneous transluminal renal artery angioplasty (PTRA) therapy improved diastolic function and cardiomyocyte hypertrophy.<sup>69</sup> MSC delivery in renal

artery stenosis decreased secretion and tissue expression of TNF- $\alpha$ , IFN- $\gamma$ , and MCP-1 and increased IL-10 compared to placebo.<sup>70</sup> Eirin et al demonstrated that a decrease in renal inflammatory markers and an increase in IL-10 was associated with increased IL-10 expression in cardiac tissue.<sup>57</sup> Furthermore, clinical trials have shown that allogeneic MSCs ameliorate chronic inflammatory responses by decreasing TNF- $\alpha$  and reversing the exhausted immune phenotype in a non-ischemic dilated cardiomyopathy population.<sup>18</sup>

Importantly, in our study, blood pressure remained within normal parameters in the combination and single-cell therapy groups compared to placebo, which may be due to a cell therapy-mediated amelioration of vasoconstriction.<sup>57</sup> Previous studies demonstrated the association of decreased TNF- $\alpha$  and microvascular remodeling.<sup>71</sup> Allogeneic MSCs restore endothelial function, as assessed by improved EPC bioactivity and flow-mediated vasodilation.<sup>23</sup> Accordingly, the placebo group, which had a marked increase in blood pressure, had a substantial proportional change in titin phosphorylation at 12 weeks, indicative of ventricular stiffness and impaired relaxation. These immunomodulatory and vascular effects<sup>16,72,73</sup> could have therapeutic importance in HFpEF, a disorder with marked chronic inflammation and endothelial dysfunction as an underlying etiology.

Taken together, ACCT improved the reparative capacity to a greater extent than single-cell therapy in various large animal studies of ICM<sup>17,25,74</sup> as well as in the recently published, double-blind, placebo-controlled clinical trial in patients with ICM, CONCERT-HF (Combination of Mesenchymal and Cardiac Stem Cells as Regenerative Therapy for Heart Failure).<sup>75,76</sup> Our study is the first to evaluate allogeneic MSCs and KSCs both in combination and as single-cell therapy in a CKD-induced HFpEF large animal model and supports the safety and feasibility of this approach.

### Limitations

Limitations of the study include the young age of the animals and lack of associated comorbidities in comparison with the patients that typically develop CKD and HFpEF. The development of HFpEF was mild due to the relatively short period of time of the study (12 weeks) and the moderate stage of the CKD. Indeed, the natural history of HFpEF associated with CKD requires longer follow-up time to evaluate the progressive remodeling of the cardiac ventricles and induction of fibrosis and extracellular matrix changes. However, swine cardiac anatomy and physiology are similar to that in humans and even mild changes translate to patients. In separate studies, we recently demonstrated that follow up for up to 18 weeks resulted in further increases in LVED mass/BSA and maintenance of significant diastolic dysfunction, assessed through hemodynamic and molecular methods, and CKD, consistent with the notion that longer follow-up results in progressive cardiac remodeling.<sup>33</sup>

### Conclusion

Renal intra-arterial delivery of allogeneic MSCs and KSCs was safe and improved renal function and ameliorated diastolic function in a large animal model of CKD-induced HFpEF. Cell therapy also prevented the increase in blood pressure over time. These findings illustrate the importance of the interaction between different populations of progenitors and the safety of ACCT, encouraging the further development

of preclinical and clinical trials in the HFpEF and CKD populations.

### Acknowledgments

The current academic affiliation of I.H.S. is as follows: Voluntary Faculty, University of Miami Miller School of Medicine, Miami, FL, USA. This work was performed while she was a Professor of Clinical Medicine at the University of Miami Miller School of Medicine, Miami, FL, USA.

### Funding

This study was funded by a generous gift from the Lipson Family and in part by a National Institutes of Health (NIH) grant, R01 HL107110, to J.M.H. J.M.H. and I.H.S. were also supported by NIH grants, 1R01 HL134558, 5UM1HL113460, and R01 HL137355 and by the Starr and Soffer Family Foundations. A.K. and J.M.H. are supported by National Heart, Lung, and Blood Institute of Health (NHLBI) grants, NHLBI-ECB-HB-2016-09-JB and 4UM1HL087318-10, as well as by Production Assistance for Cell Therapy grants, PCT0013-01, PCT0004-02, and PCT0009-01, along with the Marcus Foundation.

### Conflict of Interest

Aisha Khan discloses a relationship with AssureImmune Cord Blood Bank that includes equity. AssureImmune Cord Blood did not play a role in the design, conduct, or funding of the study. Krystaleia Valasaki discloses a relationship with Vestion Inc. that includes equity. Joshua M. Hare reports having a patent for cardiac cell-based therapy. He holds equity in Vestion Inc. and maintains a professional relationship with Vestion Inc. as a consultant and member of the Board of Directors and Scientific Advisory Board. He is the Chief Scientific Officer, a compensated consultant and advisory board member for Longeveron, and holds equity in Longeveron. He is also the co-inventor of intellectual property licensed to Longeveron. Longeveron LLC and Vestion Inc. did not participate in funding this work. His relationships are disclosed to the University of Miami, and a management plan is in place. The University of Miami is an equity owner in Longeveron, which has licensed intellectual property from the University of Miami. This manuscript was prepared by Ivonne Hernandez Schulman in her personal capacity during her time as a faculty member at the University of Miami. The opinions expressed in this article are the author's own and do not reflect the view of the National Institutes of Health, the Department of Health and Human Services, or the US government. All of the other authors declared no potential conflicts of interest.

### Author Contributions

A.C.R.: conception and design, analysis and/or interpretation, manuscript writing, collection and/or assembly of data; B.A.T., M.N., V.F., M.N.B., J.R., M.R., V.P., K.V., L.M.T., K.C., S.D., M.A.B., N.D.K., A.M.L., D.V.H., D.A.R.: collection and/or assembly of data; A.K.: administrative support; W.B.: administrative support, critical review, final approval of manuscript; J.M.H.: financial support, analysis and/or interpretation, critical review, final approval of manuscript;



I.H.S.: conception and design, financial support, analysis and/or interpretation, final approval of manuscript, critical review.

## Data Availability

The data that support the findings of this study are available from the corresponding author upon reasonable request.

## Supplementary Material

Supplementary material is available at *Stem Cells Translational Medicine* online.

## References

- Owan TE, Hodge DO, Herges RM, Jacobsen SJ, Roger VL, Redfield MM. Trends in prevalence and outcome of heart failure with preserved ejection fraction. *N Engl J Med*. 2006;355(3):251-259.
- Benjamin EJ, Muntner P, Alonso A, et al.; American Heart Association Council on Epidemiology and Prevention Statistics Committee and Stroke Statistics Subcommittee. Heart disease and stroke statistics—2019 update: a report from the American Heart Association. *Circulation*. 2019;139(10):e56-e528.
- Dunlay SM, Roger VL, Redfield MM. Epidemiology of heart failure with preserved ejection fraction. *Nat Rev Cardiol*. 2017;14(10):591-602.
- Silverman DN, Plante TB, Infeld M, et al. Association of  $\beta$ -blocker use with heart failure hospitalizations and cardiovascular disease mortality among patients with heart failure with a preserved ejection fraction: a secondary analysis of the TOPCAT trial. *JAMA Netw Open*. 2019;2(12):e1916598.
- Kjeldsen SE, von Lueder TG, Smiseth OA, et al. Medical therapies for heart failure with preserved ejection fraction. *Hypertension*. 2020;75(1):23-32.
- Solomon SD, McMurray JJV, Anand IS, et al. Angiotensin-neprilysin inhibition in heart failure with preserved ejection fraction. *N Engl J Med*. 2019;381:1609-1620.
- Daly C. Is early chronic kidney disease an important risk factor for cardiovascular disease? A background paper prepared for the UK Consensus Conference on early chronic kidney disease. *Nephrol Dial Transplant*. 2007;22(Suppl 9):ix19-ix25.
- Bignelli AT, Barberato SH, Avelas P, Abensur H, Pecoits-Filho R. The impact of living donor kidney transplantation on markers of cardiovascular risk in chronic kidney disease patients. *Blood Purif*. 2007;25(3):233-241.
- Glasscock RJ, Pecoits-Filho R, Barberato SH. Left ventricular mass in chronic kidney disease and ESRD. *Clin J Am Soc Nephrol*. 2009;4(Suppl 1):S79-S91.
- Wali RK, Wang GS, Gottlieb SS, et al. Effect of kidney transplantation on left ventricular systolic dysfunction and congestive heart failure in patients with end-stage renal disease. *J Am Coll Cardiol*. 2005;45(7):1051-1060.
- Faul C, Amaral AP, Oskouei B, et al. FGF23 induces left ventricular hypertrophy. *J Clin Invest*. 2011;121(11):4393-4408.
- Gutiérrez OM, Januzzi JL, Isakova T, et al. Fibroblast growth factor 23 and left ventricular hypertrophy in chronic kidney disease. *Circulation*. 2009;119(19):2545-2552.
- Cachofeiro V, Goicochea M, de Vinuesa SG, Oubiña P, Lahera V, Luño J. Oxidative stress and inflammation, a link between chronic kidney disease and cardiovascular disease. *Kidney Int*. 2008;74:S4-S9.
- Loffredo FS, Nikolova AP, Pancoast JR, Lee RT. Heart failure with preserved ejection fraction: molecular pathways of the aging myocardium. *Circ Res*. 2014;115(1):97-107.
- Shah SJ, Katz DH, Selvaraj S, et al. Phenomapping for novel classification of heart failure with preserved ejection fraction. *Circulation*. 2015;131(3):269-279.
- Bagno L, Hatzistergos KE, Balkan W, Hare JM. Mesenchymal stem cell-based therapy for cardiovascular disease: progress and challenges. *Mol Ther*. 2018;26(7):1610-1623.
- Natsumeda M, Florea V, Rieger AC, et al. A combination of allogeneic stem cells promotes cardiac regeneration. *J Am Coll Cardiol*. 2017;70(20):2504-2515.
- Hare JM, DiFede DL, Rieger AC, et al. Randomized comparison of allogeneic versus autologous mesenchymal stem cells for nonischemic dilated cardiomyopathy: POSEIDON-DCM trial. *J Am Coll Cardiol*. 2017;69(5):526-537.
- Florea V, Rieger AC, DiFede DL, et al. Dose comparison study of allogeneic mesenchymal stem cells in patients with ischemic cardiomyopathy (The TRIDENT Study). *Circ Res*. 2017;121(11):1279-1290.
- Heldman AW, DiFede DL, Fishman JE, et al. Transendocardial mesenchymal stem cells and mononuclear bone marrow cells for ischemic cardiomyopathy: the TAC-HFT randomized trial. *JAMA*. 2014;311(1):62-73.
- Hare JM, Fishman JE, Gerstenblith G, et al. Comparison of allogeneic vs autologous bone marrow-derived mesenchymal stem cells delivered by transendocardial injection in patients with ischemic cardiomyopathy: the POSEIDON randomized trial. *JAMA*. 2012;308(22):2369-2379.
- Hatzistergos KE, Quevedo H, Oskouei BN, et al. Bone marrow mesenchymal stem cells stimulate cardiac stem cell proliferation and differentiation. *Circ Res*. 2010;107(7):913-922.
- Premier C, Blum A, Bellio MA, et al. Allogeneic mesenchymal stem cells restore endothelial function in heart failure by stimulating endothelial progenitor cells. *EBioMedicine*. 2015;2(5):467-475.
- Quevedo HC, Hatzistergos KE, Oskouei BN, et al. Allogeneic mesenchymal stem cells restore cardiac function in chronic ischemic cardiomyopathy via trilineage differentiating capacity. *Proc Natl Acad Sci USA*. 2009;106(33):14022-14027.
- Karantalis V, Suncion-Loescher VY, Bagno L, et al. Synergistic effects of combined cell therapy for chronic ischemic cardiomyopathy. *J Am Coll Cardiol*. 2015;66(18):1990-1999.
- Karantalis V, DiFede DL, Gerstenblith G, et al. Autologous mesenchymal stem cells produce concordant improvements in regional function, tissue perfusion, and fibrotic burden when administered to patients undergoing coronary artery bypass grafting: the prospective randomized study of mesenchymal stem cell therapy in patients undergoing cardiac surgery (PROMETHEUS) trial. *Circ Res*. 2014;114(8):1302-1310.
- Amado LC, Saliaris AP, Schuleri KH, et al. Cardiac repair with intramyocardial injection of allogeneic mesenchymal stem cells after myocardial infarction. *Proc Natl Acad Sci USA*. 2005;102(32):11474-11479.
- Rangel EB, Gomes SA, Dulce RA, et al. c-Kit<sup>+</sup> cells isolated from developing kidneys are a novel population of stem cells with regenerative potential. *Stem Cells*. 2013;31(8):1644-1656.
- Gomes SA, Hare JM, Rangel EB. Kidney-derived c-Kit<sup>+</sup> cells possess regenerative potential. *Stem Cells Transl Med*. 2018;7(4):317-324.
- Rangel EB, Gomes SA, Kanashiro-Takeuchi R, et al. Kidney-derived c-kit<sup>+</sup> progenitor/stem cells contribute to podocyte recovery in a model of acute proteinuria. *Sci Rep*. 2018;8(1):14723.
- Hu K, Ertl G. A new porcine model of hypertensive cardiomyopathy: a helpful tool to explore the HFpEF mystique. *Am J Physiol Heart Circ Physiol*. 2015;309(9):H1390-H1391.
- Schwarzl M, Hamdani N, Seiler S, et al. A porcine model of hypertensive cardiomyopathy: implications for heart failure with preserved ejection fraction. *Am J Physiol Heart Circ Physiol*. 2015;309(9):H1407-H1418.
- Rieger AC, Bagno LL, Salerno A, et al. Growth hormone-releasing hormone agonists ameliorate chronic kidney disease-induced heart failure with preserved ejection fraction. *Proc Natl Acad Sci USA*. 2021;118(4):e2019835118.
- Misra S, Gordon JD, Fu AA, et al. The porcine remnant kidney model of chronic renal insufficiency. *J Surg Res*. 2006;135(2):370-379.



35. Chagnac A, Zingerman B, Rozen-Zvi B, Herman-Edelstein M. Consequences of glomerular hyperfiltration: the role of physical forces in the pathogenesis of chronic kidney disease in diabetes and obesity. *Nephron*. 2019;143(1):38-42.
36. Srivastava T, Hariharan S, Alon US, et al. Hyperfiltration-mediated injury in the remaining kidney of a transplant donor. *Transplantation*. 2018;102(10):1624-1635.
37. Siskin GP, Dowling K, Virmani R, Jones R, Todd D. Pathologic evaluation of a spherical polyvinyl alcohol embolic agent in a porcine renal model. *J Vasc Interv Radiol*. 2003;14(1):89-98.
38. Da Silva JS, Hare JM. Cell-based therapies for myocardial repair: emerging role for bone marrow-derived mesenchymal stem cells (MSCs) in the treatment of the chronically injured heart. *Methods Mol Biol*. 2013;1037:145-163.
39. Williams AR, Trachtenberg B, Velazquez DL, et al. Intramyocardial stem cell injection in patients with ischemic cardiomyopathy: functional recovery and reverse remodeling. *Circ Res*. 2011;108(7):792-796.
40. Boyle AJ, McNiece IK, Hare JM. Mesenchymal stem cell therapy for cardiac repair. *Methods Mol Biol*. 2010;660:65-84.
41. Zakeri R, Moulay G, Chai Q, et al. Left atrial remodeling and atrioventricular coupling in a canine model of early heart failure with preserved ejection fraction. *Circ Heart Fail*. 2016;9(10):e003238.
42. Müller AE, Kötter S, Krüger M, et al. Differential changes in titin domain phosphorylation increase myofibrillar stiffness in failing human hearts. *Cardiovasc Res*. 2013;99:648-656.
43. Borbély A, Falcao-Pires I, van Heerebeek L, et al. Hypophosphorylation of the Stiff N2B titin isoform raises cardiomyocyte resting tension in failing human myocardium. *Circ Res*. 2009;104(6):780-786.
44. Ponikowski P, Voors AA, Anker SD, et al.; Authors/Task Force Members; Document Reviewers. 2016 ESC Guidelines for the diagnosis and treatment of acute and chronic heart failure: The Task Force for the diagnosis and treatment of acute and chronic heart failure of the European Society of Cardiology (ESC). Developed with the special contribution of the Heart Failure Association (HFA) of the ESC. *Eur J Heart Fail*. 2016;18(8):891-975.
45. Lam CSP, Voors AA, de Boer RA, Solomon SD, van Veldhuisen DJ. Heart failure with preserved ejection fraction: from mechanisms to therapies. *Eur Heart J*. 2018;39(30):2780-2792.
46. McMurray JJV, Jackson AM, Lam CSP, et al. Effects of sacubitril-valsartan versus valsartan in women compared with men with heart failure and preserved ejection fraction: insights from PARAGON-HF. *Circulation*. 2020;141(5):338-351.
47. Tompkins BA, Rieger AC, Florea V, et al. Comparison of mesenchymal stem cell efficacy in ischemic versus nonischemic dilated cardiomyopathy. *J Am Heart Assoc*. 2018;7(14):e008460.
48. Zeng L, Hu Q, Wang X, et al. Bioenergetic and functional consequences of bone marrow-derived multipotent progenitor cell transplantation in hearts with postinfarction left ventricular remodeling. *Circulation*. 2007;115(14):1866-1875.
49. Feygin J, Mansoor A, Eckman P, Swingen C, Zhang J. Functional and bioenergetic modulations in the infarct border zone following autologous mesenchymal stem cell transplantation. *Am J Physiol Heart Circ Physiol*. 2007;293(3):H1772-H1780.
50. Bagno L, Hatzistergos KE, Balkan W, Hare JM. Mesenchymal stem cell-based therapy for cardiovascular disease: progress and challenges. *Mol Ther*. 2018;26(7):1610-1623.
51. Rangel EB, Gomes SA, Kanashiro-Takeuchi R, Saltzman RG, Wei C, Ruiz P, Reiser J, Hare JM. Kidney-derived c-kit+ progenitor/stem cells contribute to podocyte recovery in a model of acute proteinuria. *Sci Rep*. 2018;8:147238.
52. Rieger AC, Bagno L, Florea V, Schulman IH. *Stem Cell Therapies for Renal Diseases. Reference Module in Biomedical Sciences*. Elsevier; 2019.
53. Chade AR, Brosh D, Higano ST, Lennon RJ, Lerman LO, Lerman A. Mild renal insufficiency is associated with reduced coronary flow in patients with non-obstructive coronary artery disease. *Kidney Int*. 2006;69(2):266-271.
54. Ter Maaten JM, Damman K, Verhaar MC, et al. Connecting heart failure with preserved ejection fraction and renal dysfunction: the role of endothelial dysfunction and inflammation. *Eur J Heart Fail*. 2016;18(6):588-598.
55. Rauchhaus M, Doehner W, Francis DP, et al. Plasma cytokine parameters and mortality in patients with chronic heart failure. *Circulation*. 2000;102(25):3060-3067.
56. Paulus WJ, Tschöpe C. A novel paradigm for heart failure with preserved ejection fraction: comorbidities drive myocardial dysfunction and remodeling through coronary microvascular endothelial inflammation. *J Am Coll Cardiol*. 2013;62(4):263-271.
57. Eirin A, Zhu XY, Ferguson CM, et al. Intra-renal delivery of mesenchymal stem cells attenuates myocardial injury after reversal of hypertension in porcine renovascular disease. *Stem Cell Res Ther*. 2015;6:7.
58. Baumann B, Hayashida T, Liang X, Schnaper HW. Hypoxia-inducible factor-1 $\alpha$  promotes glomerulosclerosis and regulates COL1A2 expression through interactions with Smad3. *Kidney Int*. 2016;90(4):797-808.
59. Kushida N, Nomura S, Mimura I, et al. Hypoxia-inducible factor-1 $\alpha$  activates the transforming growth factor- $\beta$ /SMAD3 pathway in kidney tubular epithelial cells. *Am J Nephrol*. 2016;44(4):276-285.
60. Siragy HM, Carey RM. Role of the intrarenal renin-angiotensin-aldosterone system in chronic kidney disease. *Am J Nephrol*. 2010;31(6):541-550.
61. Saad A, Dietz AB, Herrmann SMS, et al. Autologous mesenchymal stem cells increase cortical perfusion in renovascular disease. *J Am Soc Nephrol*. 2017;28(9):2777-2785.
62. Abumowad A, Saad A, Ferguson CM, et al. In a Phase 1a escalating clinical trial, autologous mesenchymal stem cell infusion for renovascular disease increases blood flow and the glomerular filtration rate while reducing inflammatory biomarkers and blood pressure. *Kidney Int*. 2020;97(4):793-804.
63. Seeland U, Haeuseler C, Hinrichs R, et al. Myocardial fibrosis in transforming growth factor- $\beta_1$  (TGF- $\beta_1$ ) transgenic mice is associated with inhibition of interstitial collagenase. *Eur J Clin Invest*. 2002;32(5):295-303.
64. Kuwahara F, Kai H, Tokuda K, et al. Transforming growth factor- $\beta$  function blocking prevents myocardial fibrosis and diastolic dysfunction in pressure-overloaded rats. *Circulation*. 2002;106(1):130-135.
65. Borlaug BA, Olson TP, Lam CS, et al. Global cardiovascular reserve dysfunction in heart failure with preserved ejection fraction. *J Am Coll Cardiol*. 2010;56(11):845-854.
66. Iwanaga Y, Kihara Y, Hasegawa K, et al. Cardiac endothelin-1 plays a critical role in the functional deterioration of left ventricles during the transition from compensatory hypertrophy to congestive heart failure in salt-sensitive hypertensive rats. *Circulation*. 1998;98(19):2065-2073.
67. Dobaczewski M, Chen W, Frangogiannis NG. Transforming growth factor (TGF)- $\beta$  signaling in cardiac remodeling. *J Mol Cell Cardiol*. 2011;51(4):600-606.
68. Hawwa N, Shrestha K, Hammad M, Yeo PSD, Fatica R, Tang WHW. Reverse remodeling and prognosis following kidney transplantation in contemporary patients with cardiac dysfunction. *J Am Coll Cardiol*. 2015;66(16):1779-1787.
69. Urbietta-Caceres VH, Zhu XY, Gibson ME, et al. Reversal of experimental renovascular hypertension restores coronary microvascular function and architecture. *Am J Hypertens*. 2011;24(4):458-465.
70. Eirin A, Zhang X, Zhu XY, et al. Renal vein cytokine release as an index of renal parenchymal inflammation in chronic experimental renal artery stenosis. *Nephrol Dial Transplant*. 2014;29(2):274-282.
71. Zhu XY, Daghini E, Chade AR, et al. Simvastatin prevents coronary microvascular remodeling in renovascular hypertensive pigs. *J Am Soc Nephrol*. 2007;18(4):1209-1217.
72. Karantalis V, Schulman IH, Balkan W, Hare JM. Allogeneic cell therapy: a new paradigm in therapeutics. *Circ Res*. 2015;116(1):12-15.

73. Casiraghi F, Remuzzi G, Abbate M, Perico N. Multipotent mesenchymal stromal cell therapy and risk of malignancies. *Stem Cell Rev Rep.* 2013;9(1):65-79.
74. Williams AR, Hatzistergos KE, Addicott B, et al. Enhanced effect of combining human cardiac stem cells and bone marrow mesenchymal stem cells to reduce infarct size and to restore cardiac function after myocardial infarction. *Circulation.* 2013;127(2):213-223.
75. Bolli R, Hare JM, March KL, et al.; Cardiovascular Cell Therapy Research Network (CCTRn). Rationale and design of the CONCERT-HF trial (combination of mesenchymal and c-kit<sup>+</sup> cardiac stem cells as regenerative therapy for heart failure). *Circ Res.* 2018;122(12):1703-1715.
76. Bolli R, Mitrani RD, Hare JM, et al.; Cardiovascular Cell Therapy Research Network (CCTRn). A Phase II study of autologous mesenchymal stromal cells and c-kit positive cardiac cells, alone or in combination, in patients with ischaemic heart failure: the CCTRn CONCERT-HF trial. *Eur J Heart Fail.* 2021;23(4):661-674.